ON THE PRESERVATION OF THE MECHANICAL INTEGRITY OF FIBER REINFORCED COMPOSITES WITH INTEGRATED FUNCTIONS

Katharina Haag[1], Jonas Deitschun[2], Dirk Godlinski[3], Volker Zoellmer[4] and Katharina Koschek[5]

Fraunhofer Institute for Manufacturing Technology and Advanced Materials IFAM, Wiener Str. 12, D-28359 Bremen, Web Page: http://www.ifam.fraunhofer.de
[1]Email: Katharina.Haag@ifam.fraunhofer.de
[2] Email: Jonas.Deitschun@ifam.fraunhofer.de
[3] Email: Dirk.Godlinski@ifam.fraunhofer.de
[4] Email: Volker.Zoellmer@ifam.fraunhofer.de
[5] Email: Katharina.Koschek@ifam.fraunhofer.de

Keywords: Glass fiber composites; printed functionalization; interfacial shear strength; 3-point bending

Abstract
One main issue when adding extra functionalities to fiber reinforced composites is to preserve their mechanical integrity. A promising attempt with large degrees of freedom in terms of design of the integrated function displays the integration of printed structures. Examples shown here include wireless readable deformation elements, piezo sensors and heating structures. We can show that composite processing via vacuum infusion is possible without any larger adaptations in processing and that the resulting composites withstand comparable loads to the non-functionalized composites independently of the layer of integration into the composite. In contrast, integrated polymer layers of comparable size significantly decrease the apparent interfacial shear strength. The preservation of the mechanical integrity in the case of printed functionalization can be explained by good chemical compatibility of the matrix resin and the functional material (epoxy filled with metal particles). Hence, the results present a promising attempt for function-integrated composites for structural health monitoring and beyond.

1. Introduction

Fiber reinforced plastics (FRP) are widely used in aeronautics as lightweight materials to reduce fuel consumption. But large safety factors are applied in part dimensioning to meet the safety requirements for airplanes. In addition to the over-dimensioning, maintenance of FRP components is a crucial but time-consuming step and hence cost intensive. With structural health monitoring (SHM) concepts, the maintenance time and therefore the ground time of an airplane could be reduced and the safety factors applied to the dimensioning can be decreased. So, there is further room for exploitation of the lightweight potential of FRP. During the last years, significant research was performed to find reliable SHM concepts to detect critical defects in the composites structure, e.g., impact damages or delamination (see, e.g., the review by Ferreira et al. [1]). Several attempts have been developed to integrate layers with sensor networks into FRPs to detect potential damages [1-4].
Our work deals with the question of how to minimize the input of material and to avoid extra layers in the composite when integrating functions into FRP. We use digital printing techniques to directly functionalize the textile fabric with conductive paths and sensor structures prior to their integration into the polymeric matrix. We analyze the impact and the potential of printed structures within the

composite by varying the functionalized layer within the composite set-up and the covered area of the textile.

2. Material and methods

2.1 Functionalization and composite manufacturing

Glass fiber twill weaves (Type 92125, Twill 2/2, 280 g/m², P-D Interglass Technologies GmbH, Erbach, Germany) were used for composites manufacturing and as substrate for functionalization via printing. For printed functionalization a micro dispensing valve (MDV 3200A, VERMES Microdispensing GmbH, Otterfing, Germany) was used to apply the electrically conductive silver filled polymer paste (1901 SB, ESL Europe, Reading Berkshire, England). After printing, copper foil contact pads were placed into the wet paste and dried subsequently in air at 100 °C for 20 min.
The different functionalizations and settings are given in Table 1. The composite plates in the size of 30 x 30 cm² were set up out of 6 layers of the glass fiber fabric. The functionalized fabrics were put in different positions as indicated in Table 1, where L1 indicates the layer directly in the mold, L3 indicates a (printed) functionalization in the middle plane of the composite, and L6 is the top layer. Composites were fabricated using a vacuum infusion process with an epoxy resin (epoxy resin L, hardener EPH 161, both supplied by R&G Faserverbundwerkstoffe, Waldenbuch, Germany) as shown schematically in Figure 1 using a semipermeable membrane for homogeneous pressure distribution inside the composite. After curing for 24 h at room temperature, the plates were demolded and consumables were removed. A post-curing step was applied for 15 h at 110 °C in an oven (Kendro UT 20 P, Kendro Laboratory Products GmbH, Langensebold, Germany) to achieve optimum dimensional stability of the composites. 16 test samples were cut from the plates using a water cooled diamond saw (ATM Brillant 265, ATM GmbH, Mammelzen, Germany) at 2000 turns/min and a feed rate of 5mm/s. The peel ply was removed from the cut samples prior to further treatment.
The contact pads attached to the printed heating structures were made accessible using a dremel (Dremel 400 Series, Robert Bosch Power Tools GmbH, Leinfelden-Echterdingen, Germany) and cables were attached via brazing. The electrical resistance was checked using a multimeter (289 True RMS Multimeter, Fluke Deutschland GmbH, Glottetal, Germany).

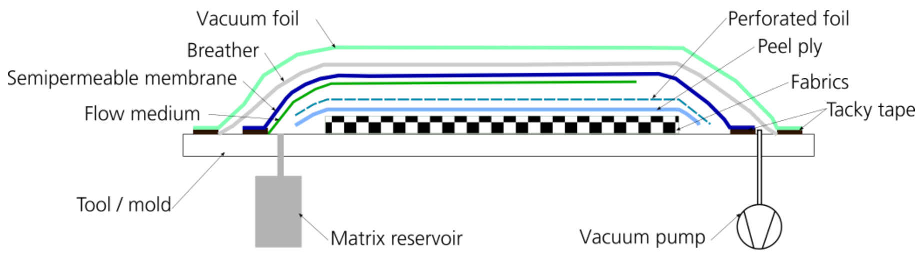

Figure 1. Schematic representation of the vacuum infusion set up used for composite manufacturing. © Fraunhofer IFAM

Samples from Type 1, 4a and 5a were arranged within the plate as shown in Figure 2A, samples from type 4b and 5b in Figure 2B. In both set-ups, non-functionalized samples are arranged in between the functionalized ones to enable a comparison of the mechanical properties and excluding potential manufacturing induced variation between different plates.
The area covered by the functionalization in samples of type 4a, 4b, 5a and 5b was calculated as size of the functionalization (length x width) divided by the sample are (length x width).

Table 1. Functionalizations applied to glass fiber fabrics prior to their integration into the composite.

Type	Functionalization	*Layout*	*Printing material & parameters*	*Integrated layer in the GFRP*
1	Heating structure	Meander structures of 10 mm width and 100 mm length, copper foil contact pads (5 mm diameter) attached to the ends of the meander	Silver filled ESL 1901 SB paste applied with Vermes MDV 3200 A print head; track width ~0.8 mm and height of ~70 µm.	L1, L3, L4, L6
2	Wireless readable deformation element	Snail-shaped printing: 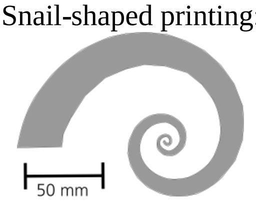	Same material as for type 1. For forming a fully filled area, 10 % overlap of the tracks was used.	L6
3	Piezo sensors	Three layer layout: bottom electrode, piezo layer, top electrode	Both electrodes were printed like 2. For the piezo layer, a PTZ filled polymer was used applied with the same print head.	L6
4a	Printed areas	Sample size 120 x 25 mm²; printed areas of 100 mm length; 1, 2, 4, 8, 16 and 32 parallel lines were printed 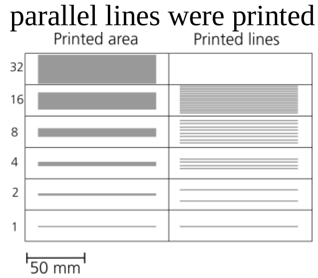	Same parameters as for type 1; samples were printed both with 10 % overlap of the lines leading to a filled area and with a distance between the lines leading to separate lines (2-16 lines only).	L3
4b		Sample size 20 x 10 mm²; printed areas of 15 mm length and 2, 4, 6 and 8 mm width	Same as for Type 4a	L3
5a	Integrated PTFE sheets	Sample size 120 x 25 mm²; PTFE foils of 100 mm length and 2, 4, 6, 8, 12, 20 mm width	PTFE foil (0.13 mm thickness, self-adhesive, Type 340050000S, Arthur Krüger GmbH, Barsbüttel, Germany) was attached to the glass fabric	L3
5b		Sample size 20 x 10 mm²; PTFE foils of 15 mm length and 2, 4, 6 and 8 mm width	Same as for type 5a	L3

were integrated

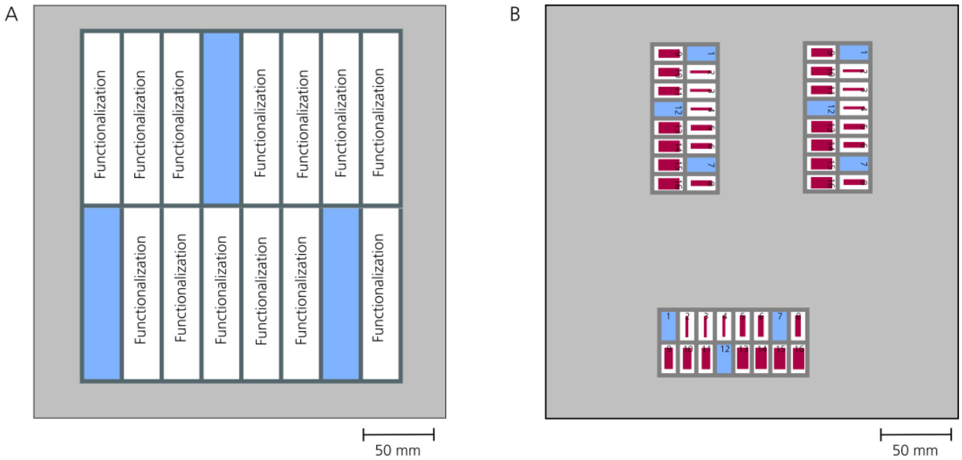

Figure 2. Sample arrangements within the manufactured plates. A) Sample types 1, 4a and 5a; B) sample types 4b and 5b. Blue fields label the position of reference samples.

2.2 Mechanical characterization

The composite samples of type 1, 4a and 5a were tested in three point bending tests based on DIN EN ISO 14125 A [5]; the bending strength σ_f in MPa and bending modulus E_f in MPa were calculated according to Eq. 1 and 2, respectively. The apparent interlaminar shear strength τ in MPa was determined according to DIN EN 2563 [6] from samples of type 4b and 5b (Eq. 3). The details of the test set-ups are given in Table 2.

$$\sigma_{max} = \frac{3\ F_{max} l_v}{2\ B\ H^2} \tag{1}$$

$$E_f = \frac{{l_v}^3}{4\ B\ H^3}\left(\frac{\Delta F}{\Delta s}\right). \tag{2}$$

With: B: width of the sample in mm; H: thickness of the sample in mm; F_{max}: maximum load in N; l_v: distance between supports in mm; Δs: difference between the deformation s'' = 3 mm and s' = 1 mm; ΔF: difference between the corresponding loads at the deformation s'' and s'.

$$\tau = \frac{3P_r}{4\ B\ H} \tag{3}$$

With: P_r: maximum load at the moment of first failure in N.

Table 2. Testing parameters for mechanical characterization of the composite samples.

	3-point bending experiments based on DIN EN ISO 14125A	Determination of the apparent interlaminar shear strength according to DIN EN 2563
Sample size in mm (length L x width B x height H)	120 x 25 x 1.5	20 x 10 x 1.5
$r1$ (upper role) in mm	5	3
$r2$ (two support roles) in mm	5	3
Distance between supports l_v in mm	80	10
Displacement rate in mm/min	1	1

3. Results and discussion

3.1. Integrated functions

Digital printing techniques were applied to functionalize glass fiber fabrics prior to their integration into the FRP via vacuum infusion. An overview of integrated functions is given in Figure 3. We can show that a set of different printed functionalities withstands the applied composite manufacturing process in terms of handling of the functionalized semi-finished products, position stability, functionality and processability with vacuum infusion. The integrated functionalities cover a wide range of applications for SHM (piezo sensors [7], wireless readable deformation element, conductive paths to contact the piezo sensors) and show further fields of use e.g. by integrating heating structures.

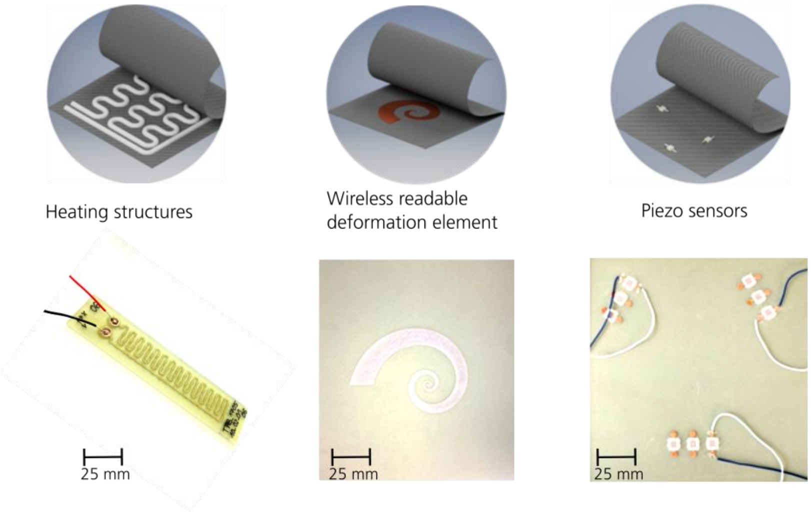

Figure 3. Overview of functions integrated into the composite. Heating structures (left), a wireless readable deformation element (middle) and piezo sensors (right) were successfully integrated into GFRP.

3.2. FRP Manufacturing with functionalized fabrics and their functionality

From a processing point of view, cautious handling of semi-finished products, especially of twill and satin weaves, is common [8]. The functionalized textiles were handled similarly without further challenges in setting up the composite set up. A full infiltration could be realized using a standard vacuum infusion process with a semipermeable membrane for all integrated functions (see Fig. 3). The larger the printed structure (e.g. larger scale wireless readable deformation sensors), the more care has to be taken to ensure a complete infiltration of the lay-up. This can be realized by an adapted flow channel management enabling a complete impregnation to avoid porosity within the composite.

By post-curing the composite structure, the electrical resistance of conductive paths is decreased, leading to a higher efficiency of the integrated structures. The electrical resistance showed a decrease of 48 % ± 12 % (n = 35) for the integrated heating structures compared to the printed structures on the dry textiles. This phenomenon of better conductivity after thermal treatment (as the curing of the composites after vacuum infusion) was already described e.g. for metal filled epoxy based adhesives by Lovinger [9] and Klosterman et al. [10].

The functionalization withstands larger deformation as exemplarily shown for a heating structure in 3-point-bending test, where simultaneously the electrical resistance of the functionalization was logged. The conductivity stays relatively constant during deformation of the sample up to the final failure of the composite (Fig. 4). This result seems to be independent of the position of the functionalized layer.

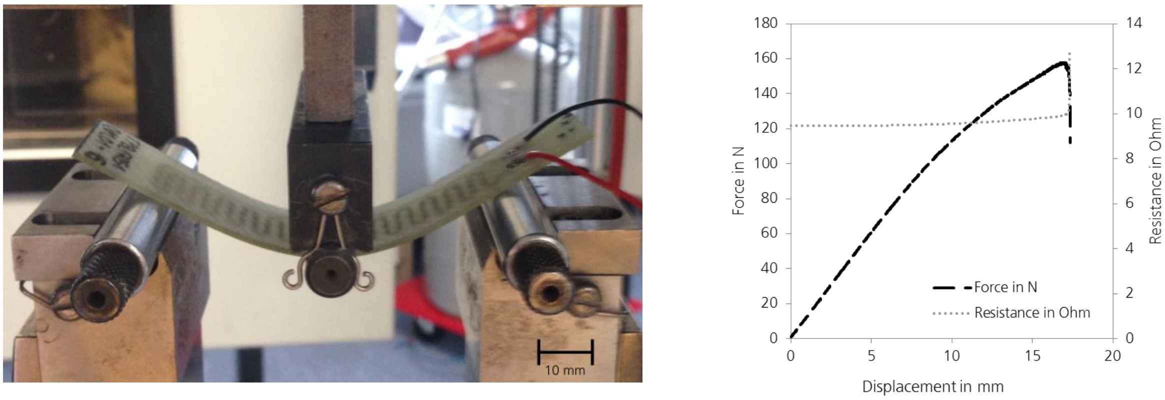

Figure 4. Composite with integrated heating structure under bending and its force-deformation curve from 3-point-bending experiments and electrical resistance of the integrated structure during deformation until fracture of the composite.

3.3. Influence of printed structures on the mechanical performance of the FRP

3 point-bending experiments of the composites with integrated heating structures did not only show conductivity up to the total failure of the composites, but as well no influence on the mechanical performance could be determined independently of the position of the integrated heating structure (see Fig. 5).

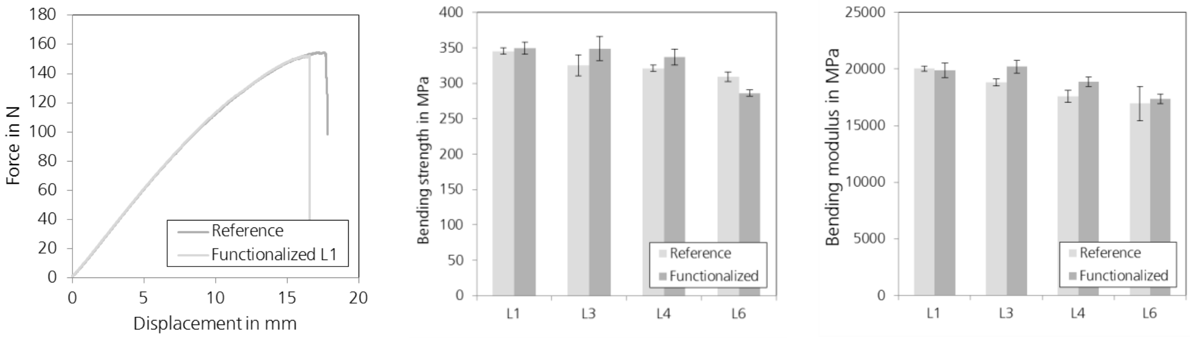

Figure 5. Influence of printed heating structures in different layers on the 3-point-bending behavior of GFRP. (A) Exemplary stress strain curves; (B) bending strength; (C) bending modulus. The mean values ± standard deviation of bending strength and modulus are given.

For a better understanding of whether or not the integrated functionalities disturb the mechanical integrity of the composites and to determine a maximum covered area without influence, printed areas and lines (type 4a, see Table 1) were compared to PTFE sheets of different size (type 5a, see Table 1) integrated into L3. With a maximum shear stress concentration in the middle plane of the composite [11], the risk of failure by delamination is maximized by positioning the functionalized layer there. The bending strength, bending modulus and apparent interlaminar shear strength of the functionalized samples with printed areas and PTFE sheets are shown in Figure 6.

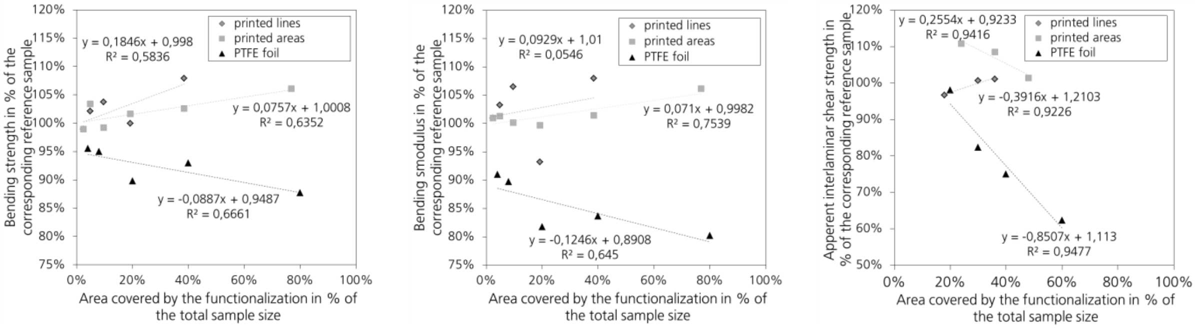

Figure 6. Influence of printed functionalization on the bending strength (A), bending modulus (B) and apparent interlaminar shear strength (C). Relative values compared to the reference samples are given. The dashed lines show the linear correlation between the area covered by the functionalization and the bending strength / modulus / apparent interfacial shear strength. The equations for the correlations and the coefficient of determination R^2 are given.

For the integrated PTFE sheets, with an increase of the sheet size a significant decrease in apparent interlaminar shear strength and as well in bending strength and modulus is visible. This can be explained by the limited adhesion between the layers 3 and 4 in the middle of the composite where load transfer via shear is only possible via friction between the composite and the PTFE sheet (which is very low). The interaction between the printed surface and the matrix of the composite is much higher leading to no significant decrease in interlaminar shear strength independently of the covered area. For the bending properties as well, no influence of the printed functionalizations on bending strength and modulus could be detected, whereas PTFE integrated samples showed a decrease. Whether these experimental results from quasi-static testing can be found as well under dynamic loads, will be tested in ongoing measurements.
Digitally printed functionalities on glass fabrics proved to give stable and functional FRPs. That gives access to large degree of freedom for the construction and manufacturing of mechanically stable composites with integrated printed functionalities especially compared to integrated functions based on polymer foils integrated into the composites [4; 12-14].

4. Conclusions

We could show that:

- A set of different functionalizations, e.g., conductive paths, sensors or antennae, directly printed on glass textiles withstand standard composite manufacturing processes (resin infusion, curing at elevated temperatures).
- The functionalizations can withstand large deformation up to the failure of the composite.
- The integration of printed structures does not affect FRP mechanical performance. This can be explained by good chemical compatibility of the functionalization and the overall matrix of the FRP.
- Large degrees of freedom for the design of integrated functions exist leading to numerous applications. Besides SHM applications, functional integration via the printing on semi-finished textiles can be transferred to further applications, e.g., the internal heating of fuselage or of the wings to avoid icing.

Acknowledgement
This work has been performed in the frame of the Fraunhofer Leitprojekt GoBeyond 4.0 “Digitale Fertigung in der Massenproduktion”, TP “Smart Wing”.
We acknowledge Katrin Greta Hoffmann for her assistance during composites manufacturing and the experiments.

References

[1] A.D.B.L. Ferreira, P.R.O. Nóvoa, A.T. Marques. Multifunctional Material Systems. A state-of-the-art review. *Composite Structures* 151:3-35, 2016.

[2] M. Lin, F.-K. Chang. The manufacture of composite structures with a built-in network of piezoceramics. *Composites Science and Technology* 62 (7-8):919–939, 2002.

[3] D. Boll, K. Schubert, C. Brauner, W. Lang. Miniaturized Flexible Interdigital Sensor for In Situ Dielectric Cure Monitoring of Composite Materials. *Sensors* 9140-2013.R1:1-6, 2013.

[4] M. Hübner, W. Lang and G. Dumstorff. Surface Integrated Printed Interdigital Structure for Process Monitoring the Curing of an Adhesive Joint. *Proceedings of the XXXI Eurosensors 2017, Paris, France*, September 3-6 2017.

[5] DIN EN ISO 14125: 2011: fibre-reinforced plastic composites – Determination of flexural properties (ISO 14125:1998 + Cor.1:2001 + Amd.1:2011); German version EN ISO 14125:1998 + AC:2002 + A1:2011.

[6] DIN EN 2563:1997: Aerospace series – Carbon fibre reinforced plastics – Unidirectional laminates – Determination of the apparent interlaminar shear strength; German version EN 2563:1997.

[7] M. Kreienborg. *Entwicklung und Analyse von hybriden Prozessketten zur drucktechnischen Sensorintegration für die Herstellung von 3D-Bauteilen aus Faserverbundwerkstoffen.* Master thesis, University of Bremen, Faculty 04: Production Engineering, 2018.- *in German.*

[8] D. Coupé. Woven reinforcements for composites. In: P. Boisse (Ed.). *Composite Reinforcements for optimum performance*. Woodhead Publishing in Materials, 2011, pp. 89-115.

[9] A.J. Lovinger. Development of Electrical conduction in silver-filled epoxy adhesives. *The Journal of Adhesions* 10:1:1-15, 1979.

[10] D. Klosterman, L. Li and J.E. Morris. Materials Characterization, Conduction Development, and Curing Effects on Reliability of Isotropically Conductive Adhesives. *IEEE Transactions on Components, Packaging, And Manufacturing Technology – Part A*, 21(1): 23-31, 1998.

[11] H. Schürmann. *Konstruieren mit Faser-Kunststoff-Verbunden*. 2nd Edition, Springer, 2007.- *in German.*

[12] G. Dumstorff and W. Lang. Printed Sensors for Material Integrated Sensing: Functionalization of Semi-Finished Parts. *Proceedings of the XXXI Eurosensors 2017, Paris, France*, September 3-6 2017.

[13] M. Hübner and W. Lang. Online Monitoring of Composites with a Miniaturized Flexible Combined Dielectric and Temperature Sensor. *Proceedings of the XXXI Eurosensors 2017, Paris, France*, September 3-6 2017.

[14] Y.Xiao, W. Qiao, H. Fukuda and H. Hatta. The effect of embedded devices on structural integrity of composite laminates. *Composite Structures*, 153:21-29, 2016.